

---

# Aggregating Gradients in Encoded Domain for Federated Learning

---

Dun Zeng<sup>1</sup> Shiyu Liu<sup>1</sup> Zenglin Xu<sup>2</sup>

## Abstract

Malicious attackers and an honest-but-curious server can steal private client data from uploaded gradients in federated learning. Although current protection methods (e.g., additive homomorphic cryptosystem) can guarantee the security of the federated learning system, they bring additional computation and communication costs. To mitigate the cost, we propose the FedAGE framework, which enables the server to aggregate gradients in an encoded domain without accessing raw gradients of any single client. Thus, FedAGE can prevent the curious server from gradient stealing while maintaining the same prediction performance without additional communication costs. Furthermore, we theoretically prove that the proposed encoding-decoding framework is a Gaussian mechanism for differential privacy. Finally, we evaluate FedAGE under several federated settings, and the results have demonstrated the efficacy of the proposed framework.

## 1. Introduction

Federated Learning (FL), a new distributed learning framework, enables multi-institutions to train machine learning models collaboratively without privacy leakage (McMahan et al., 2017; Kairouz et al., 2019; Yang et al., 2019). Typically, clients in FL system are required to upload gradients. However, FL faces many security vulnerabilities (Bhagoji et al., 2019), such as model poisoning, Byzantine attack, etc. Recent gradient inversion studies (Zhao et al., 2020; Zhu & Han, 2020; Yin et al., 2021) show how to restore private data from gradients. Consequently, such gradient inversion techniques have called for an urgent need of protection techniques in federated learning. This paper mainly focuses on defending against gradient stealing, that is, malicious

attackers and an honest-but-curious server stealing private information from the uploaded gradients.

To protect the private gradients of clients, existing modern cryptography technologies have been used to guarantee the security. Secure Multi-Party Computation (Yao, 1986) works perfectly in the cross-silo setting (i.e., a few institutions with sufficient computation and communication resources). Homomorphic Encryption (Gentry, 2009; Paillier, 1999) allows certain mathematical operations to perform directly on cipher-texts without prior decryption. However, these techniques will not only bring significant overhead to computation and communication, but also damage the efficiency of FL systems, especially cross-device scenarios. For example, when homomorphic encryption is enabled in the FL system (Zhang et al., 2020), the iteration time is extended by 135 $\times$  and the communication consumption is 13.1 GB but only 85.89 MB is needed without homomorphic encryption.

To mitigate the cost for gradient protection, we propose a practical framework named as FedAGE in this work, which *enables gradients to be aggregated in an encoded domain for federated learning*. Inspired by the paradigm of additive homomorphic cryptosystem (Paillier, 1999), we aim to build encoding-decoding strategies to aggregate gradients in a resource-friendly way. In the meantime, we hope to hide raw gradients from network providers and the FL server, since gradients are highly related to private data. To the best of our knowledge, there are two major challenges to achieve this goal: (1) ensuring encoding-decoding errors will not damage the model performance, and (2) making encoder-decoder adaptive to changing distributions and magnitudes of gradients. To address these challenges, we present a set of strategies to pretrain an error-bounded and adaptive encoder-decoder network for encoded gradients aggregation.

Furthermore, the well-pretrained encoder-decoder network can be easily deployed in federated learning procedure as illustrated in Figure 1. In practice, clients hold encoder network  $E_c$  that encodes to-be-upload gradients to prevent malicious attackers from getting raw gradients (e.g., monitor network communication). The FL server holds decoder network  $D_c$  to reconstruct aggregated gradients from the encoded domain without seeing any single client gradients. Furthermore, We theoretically demonstrate that the errors

---

<sup>1</sup>School of Computer Science and Engineering, University of Electronic Science and Technology of China <sup>2</sup>School of Computer Science and Technology, Harbin Institute of Technology Shenzhen. Correspondence to: Dun Zeng <zeng-dun@std.uestc.edu.cn>, Shiyu Liu <shyu.liu@foxmail.com>, Zenglin Xu <xuzenglin@hit.edu.cn>.

brought by the reconstructed gradients are bounded and adjustable. Especially, we prove FedAGE implements a Gaussian mechanism for differential privacy in an alternative way. Empirical evaluation has demonstrated that FedAGE maintains the prediction performance of FL models, while providing the protection to gradient information.

In short, the contributions can be summarized as follows.

- We propose the FedAGE framework with convergence guarantees, which enables the FL server to accurately aggregate gradients in an encoded domain.
- FedAGE protects the privacy of gradients by implementing a Gaussian mechanism for differential privacy via the encoder-decoder network.
- Intensive evaluation has demonstrated the good performance under both IID and Non-IID data partitions. Furthermore, experiments of differential attacks on encoded gradients show that FedAGE can prevent malicious attackers from stealing the raw gradients.

## 2. Background & Related Works

**Federated Learning.** Federated learning is a distributed learning framework, which aims to learn models across multiple participants on their local dataset. Current federated optimization strategies follow a basic pattern, which is global gradient descent according to the weighted average of uploaded gradients from clients. FedAvg (McMahan et al., 2017) aggregates model parameters trained across multiple clients based on the quantities of local data. FedProx (Li et al., 2020a) adds a proximal term into local loss functions to restrict their updates to be close. q-FedAvg (Li et al., 2020b) dynamically adjusts averaging weights for fairness concerns. As FedAvg is the representative of the weighted average optimization paradigm, we focus on the effect of our framework on FedAvg.

However, recent studies reveal that federated aggregation schemes are still suffering from privacy leakage. Previous gradient inversion researches (Zhao et al., 2020; Zhu & Han, 2020; Yin et al., 2021) demonstrate that malicious attacker can restore private data samples from gradients. It suggests a vital challenge for federated learning: *the protection methods of privacy gradients from malicious attackers and an honest-but-curious server*. There are modern cryptography strategies (e.g. Secure Multi-Party Computation (Yao, 1986) and Homomorphic Encryption (Gentry, 2009)) to guarantee the security of FL system. However, enormous resource consumption of deploying these techniques is a major obstacle, especially for resource-limited cross-device scenarios. Therefore, resolving the conflicts between the resource cost and gradients protection is another challenge.

We focus on defending against gradient inversion attack in this work, that is, preventing malicious attackers and an honest-but-curious server from stealing raw gradients of any single client. To some extent, FedAGE is a privacy-preserving framework for federated learning.

**Differential Privacy.** Differential Privacy (DP) is the state-of-the-art method for quantifying and limiting information disclosure about individuals, by introducing a level of uncertainty into the released model sufficient to mask the contribution of any individual user (Dwork & Roth, 2014). As a resource-friendly privacy protection scheme, DP has been deployed by corporations such as Google, Apple and Microsoft (Cormode et al., 2018). Abadi et al. (2016) introduces DP into deep learning procedure to protect the gradients. For federated learning, Wei et al. (2020) studies the influences of adding DP noise to federated optimization. Truex et al. (2020); Triastcyn & Faltings (2019) add different noise to meet specific DP properties.

We prove that FedAGE implements a Gaussian mechanism for DP via an additional encoding-decoding scheme in an alternative way. The encoding-decoding scheme enables the gradient aggregation in an encoded domain, and thus it can be robust to malicious gradient stealing, as verified in Section 4.1.

**Quantization.** QSGD (Alistarh et al., 2017) is a lossy gradients compression algorithm, which replaces the element of gradients with a lower number of bits (e.g., float32 to float8). Quantization techniques are popular in distributed learning for gradients compressing (Seide et al., 2014; Basu et al., 2020; Lin et al., 2018; Amiri et al., 2020).

Different from above researches, we use the quantization to map the real number vectors to the integer domain. In other words, quantization builds a connection between the real number domain and a limited integer domain. In this way, quantization limits the input domain for encoder network.

**Autoencoder.** Autoencoder is an approach to automatically learn feature representations from data. Typically, researchers use encoder network to learn a mapping from high-dimensional observations to a lower-dimensional representation space. And then, the original observations can be reconstructed from the lower-dimensional representation by decoder network. Abrahamyan et al. (2021) designs an autoencoder for extracting gradient correlation in distributed learning workers. The autoencoder enables workers to transmit similar gradients once for gradient compression. However this method does not apply to FL system due to privacy restrictions. Li & Han (2019) presents an autoencoder for gradient encryption, which however can not process changing magnitude of gradients over training process. Therefore, it brings unacceptable performance loss to models. Meanwhile, there are no mathematical guarantees

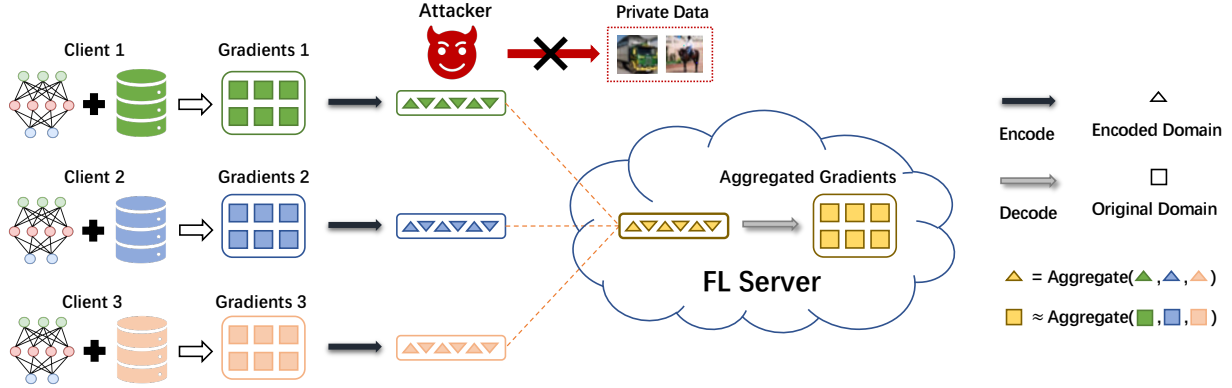


Figure 1. Overview of FedAGE. A example FL system with 3 clients and 1 server follows FedAGE. Client uploads the encoded gradients. Server collects encoded gradients from clients and aggregates them directly. Finally, server decodes gradients for global model update.

presented.

Inspired by these studies, we present a number of strategies to build an encoder-decoder network for enabling gradients to be aggregated in an encoded domain directly. Aggregation results can be reconstructed from the domain. We provide theoretical analyses of encoding-decoding errors, which are bounded and adjustable in practical applications. To the best of our knowledge, the computation cost on a tiny network is lower than that of a homomorphic cryptosystem. In addition, our encoder-decoder network is designed to bring no additional communication overhead to a FL system. We focus on evaluating the impacts of this work on FL model performance rather than its computation and communication overhead.

### 3. FedAGE: Aggregating Gradients in Encoded Domain

In this section, we present FedAGE. Firstly, we set up the to-be-solved problem in Section 3.1. Then we describe the details of pretraining autoencoder for encoded gradient aggregation in Section 3.2. Next, we introduce the procedure of applying encoder-decoder network to federated learning algorithm in Section 3.3. In Section 3.4, we theoretically analyze the mathematical properties of FedAGE.

#### 3.1. Problem Setup

Original federated optimization algorithm FedAvg minimizes finite-sum objective by averaging local model parameters collected from  $m$  clients:

$$\min_{\mathbf{w} \in \mathbb{R}^d} f(\mathbf{w}), \text{ where } f(\mathbf{w}) = \frac{1}{m} \sum_{i=1}^m \lambda_i f_i(\mathbf{w}_i; \mathcal{D}_i), \quad (1)$$

and  $f_i(\mathbf{w}; \mathcal{D}_i)$  is the loss of prediction on local dataset  $\mathcal{D}_i$ . Typically,  $\lambda_i$  represents the importance of the  $i$ -th client. As

we don't discuss the impact of weights  $\lambda$  in this paper, we simply set  $\lambda = 1$  without any preference.

Each round of FedAvg procedure runs as follow: firstly, server selects a random subset of users  $C^t$  and broadcasts global model  $\mathbf{w}^{t-1}$  to them. Next, each client  $i \in C^t$  lets  $\mathbf{w}_i^t = \mathbf{w}^{t-1}$  and performs  $k$  epochs of local stochastic gradient descent with learning rate  $\eta$  and local dataset  $\mathcal{D}_i$ . For the  $j$ -th epoch, the  $i$ -th client performs:

$$\mathbf{w}_i^t = \mathbf{w}_i^{t-1} - \eta \nabla f_{i,j}(\mathbf{w}_i^t; \mathcal{D}_i). \quad (2)$$

Then, the  $i$ -th client uploads the local gradients  $\Delta \mathbf{w}_i^t = \frac{\mathbf{w}_i^t - \mathbf{w}_i^{t-1}}{\eta}$ . Finally, the server updates global model parameters by:

$$\mathbf{w}^t = \mathbf{w}^{t-1} + \eta \sum_{i=1}^m \frac{1}{m} \Delta \mathbf{w}_i^t. \quad (3)$$

To simplify our description, we assume that the gradients  $\Delta \mathbf{w}$  and model parameters  $\mathbf{w}$  are denoted by a vector (flattened), i.e.,  $\Delta \mathbf{w}, \mathbf{w} \in \mathbb{R}^d$ .

Previous researches (Zhao et al., 2020; Zhu & Han, 2020; Yin et al., 2021) reveal that uploaded gradients may leak private data. To avoid gradients leakage, our motivation is to aggregate the gradients directly in the encoded domain. Therefore, the encoder-decoder that meets specific properties is required. Formally,  $E_c : \mathbb{R}^d \rightarrow \mathbb{R}^h$  denotes encoder function and  $D_c : \mathbb{R}^h \rightarrow \mathbb{R}^d$  denotes decoder function. For an ideal encoder-decoder pair  $(E_c^*, D_c^*)$ , the following equation should hold:

$$\forall \mathbf{x}_{1,\dots,m} \in \mathbb{R}^d, \frac{1}{m} \sum_{i=1}^m \mathbf{x}_i = D_c^* \left( \frac{1}{m} \sum_{i=1}^m E_c^*(\mathbf{x}_i) \right), \quad (4)$$

where  $m$  is the number of vector. By deploying above encoder-decoder into FedAvg procedure, we can rewrite

optimization Equation (3) as:

$$\mathbf{w}^t = \mathbf{w}^{t-1} + \eta D_c^* \left( \sum_{i=1}^m \frac{1}{m} E_c^* (\Delta \mathbf{w}^{t-1}) \right). \quad (5)$$

In practice, clients encode local gradients by  $E_c^*(\nabla f(\mathbf{w}))$ , then send encoded gradients to FL server. The server collects all clients' encoded gradients and obtains the aggregated gradients by  $D_c^* \left( \sum_{i=1}^m \frac{1}{m} E_c^* (\nabla f_i(\mathbf{w})) \right)$  directly without knowing raw gradients of any single client.

If the  $(E_c^*, D_c^*)$  does nothing to gradients that  $E_c^*(\mathbf{x}) = \mathbf{x}$ ,  $D_c^*(\mathbf{x}) = \mathbf{x}$ , then the Equation (5) degenerates to FedAvg. In this paper, we take  $h < d$  to remove redundant information of input vector via  $(E_c, D_c)$ . Inspired by the efficient gradients compression autoencoders presented by (Abrahamyan et al., 2021; Li & Han, 2019), we use an autoencoder network to fit the target encoder-decoder function. However, the observation of (Shi et al., 2019) indicates that *the magnitude of gradients decreases over the training process, and the distribution of gradients varies with neural network architectures*. For instance, the gradients distribution of ResNet-20 (He et al., 2016) is more like Normal distribution, while VGG-16 (Simonyan & Zisserman, 2015) is more like T distribution. Furthermore, the largest gradient of VGG-16 is 10 times smaller than ResNet-20.

All in all, to build an practical encoder-decoder, we are facing two main challenges in this paper:

**(1) Error-bounded.** It is difficult to build the lossless encoder-decoder pair  $(E_c^*, D_c^*)$ . Therefore, we concentrate to build an error-bounded encoding-decoding scheme. In other words, the encoding-decoding errors of  $(E_c, D_c)$  should not damage model performance.

**(2) Adaptability.** As the distribution and magnitude of gradients vary with several factors (e.g. model architectures, dataset, and hyper-parameters), the strategies for the encoder-decoder dealing with various magnitude and distribution of gradients can be tricky. In summary, it is challenging to build a general encoding-decoding strategy adaptive to changing gradients.

### 3.2. Encoded Domain Aggregation

This part is to demonstrate our strategies for building an error-bounded and adaptive encoder-decoder network  $(E_c, D_c)$  for encoded domain aggregation. Firstly, we introduce the quantization technique to limit the input domain for the encoder. And then, we describe how to pretrain encoder-decoder simultaneously for encoded domain aggregation.

**Quantization.** Different from quantization for compression researches, we use quantization to limit the input domain from  $\mathbb{R}^d$  to  $\mathbb{Z}^d$ , which makes FedAGE adaptive to changing gradients. QSGD (Alistarh et al., 2017) is popular in dis-

tributed learning, replacing element of gradients with lower number of bits. We summarise the stochastic quantization in Appendix A.

We define the quantization function  $Q(\mathbf{x}, s, n) = \mathbf{l}$ , where  $n$  is hyper-parameter for normalization,  $s \geq 1$  is the quantization level,  $\mathbf{x} \in \mathbb{R}^d$  and  $\mathbf{l} \in \mathbb{Z}^d$ . For all  $0 \leq k < d$ , the  $k$ -th element  $0 \leq l^k \leq s$  is a stochastic integer corresponding with real-value  $x^k$ . Stochastic quantization can be naively applied to federated aggregation without pre-dequantizing in server. We describe this procedure as:

$$\frac{n}{s} \frac{1}{m} \sum_{i=1}^m Q(\mathbf{x}_i; s, n) \triangleq \frac{1}{m} \sum_{i=1}^m \mathbf{x}_i, \quad (6)$$

where  $\mathbf{x}_1, \dots, \mathbf{x}_m \geq 0$ . In practice, hyper-parameters (i.e.,  $n, s, m$ ) are assigned before each FL round starts, and only the results of  $Q(\mathbf{x}_i; s, n)$  (i.e.,  $\mathbf{l}_i$ ) will be transmitted through communication network.

For better mathematical description, we define the quantified integer domain as  $\mathbb{Q}_s^d$ . For all  $\mathbf{l} \in \mathbb{Q}_s^d$  and  $0 \leq k < d$ , we have  $0 \leq l^k \leq s$ . The quantified domain  $\mathbb{Q}_s^d$  is a limited integer domain (i.e.,  $\mathbb{Q}_s^d \subseteq \mathbb{Z}^d$ ). Therefore, the quantization function maps gradients from a large real number domain  $\mathbb{R}^d$  to a quantified domain  $\mathbb{Q}_s^d$ . The quantization level  $s$  and input size  $d$  leverage the size of quantified domain, i.e., larger quantization level  $s$  and input size  $d$  lead to larger quantization domain.

**Encoded Domain Aggregation with Autoencoder.** The quantization function limits the input domain into  $\mathbb{Q}_s^d$  in our previous analyses. We use an encoder network to fit encode function  $E_c : \mathbb{Q}_s^d \rightarrow \mathbb{R}^h$  and a decoder network to fit decode function  $D_c : \mathbb{R}^h \rightarrow \mathbb{Q}_s^d$ . We train  $(E_c, D_c)$  end-to-end based on objective function below:

$$\arg \min_{E_c, D_c} \mathcal{L} \left( D_c \left( \frac{1}{m} \sum_{i=1}^m E_c(\mathbf{l}_i) \right), \sum_{i=1}^m \mathbf{l}_i \right), \quad (7)$$

where  $\mathbf{l} \in \mathbb{Q}_s^d$  and  $\mathcal{L}(\cdot, \cdot)$  is the loss function leveraging the distance between encoding-decoding outputs and ground-truth values. As the input domain is limited, the encoder-decoder network  $(E_c, D_c)$  can be pretrained with a synthetic dataset randomly generated from  $\mathbb{Q}_s^d$ . Therefore, the pretrained encoder-decoder is based on input size  $d$ , quantization level  $s$ , and the number of vectors  $m$  (i.e., the number of clients).

To the best of our knowledge, well-pretrained  $(E_c, D_c)$  can not be lossless. Therefore, we use a variable  $\boldsymbol{\nu}$  to denote the encoding-decoding errors:

$$\boldsymbol{\nu} \triangleq D_c \left( \frac{1}{m} \sum_{i=1}^m E_c(\mathbf{l}_i) \right) - \frac{1}{m} \sum_{i=1}^m \mathbf{l}_i. \quad (8)$$

To put it simply, encoder  $E_c$  learns hidden representations

(encoding) of integer vector  $l$ . Decoder  $D_c$  leverages aggregated result of  $m$  encoded vectors and decodes the corresponding aggregation results. However, encoder-decoder introduces a variance  $\nu$  between the decoding results and ground-truth values. To sum up, encoded domain aggregation strategies consist of three steps. Firstly, it uses the quantization function to map real number vectors to integer vectors. Then, the well-pretrained encoder-decoder network encodes the integer vectors, aggregates the encoded vectors directly, and reconstructs aggregated results from the quantified domain. Finally, averaged results of original vectors can be obtained by dequantizing the outputs of the decoder network. Above procedures bring encoding-decoding errors  $\nu$ . Our further theoretical analysis of errors is presented in Section 3.4 and Section 4.2.

### 3.3. Federated Encoded Gradients Aggregation

In this section, we present the FedAGE framework by summarizing Equations (3), (6) and (8). Formally, we have:

$$\frac{n}{s} D_c \left( \frac{1}{m} \sum_{i=1}^m E_c(Q(\Delta \mathbf{w}_i, s, n)) \right) = \sum_{i=1}^m \Delta \mathbf{w}_i + \frac{n}{s} \nu.$$

Without loss of generality, we apply the proposed framework to FedAvg. The details are depicted in Algorithm 1. It is important to note that FedAGE can be applied to other weighted average-based algorithms such as FedProx, q-FedAvg, etc. For example, the contents of the yellow part in Algorithm 1 can be replaced by the proximal term of FedProx. For another example, if gradients in the  $i$ -th client are multiplied by a weight  $\lambda_i$  (i.e., the blue part in Algorithm 1) before inputting it into the encoder network, we can achieve dynamically weighted average like q-FedAvg.

In practice, we perform encoding-decoding procedure on positive and negative gradients respectively. In other words, the  $(E_c, D_c)$  processes negative gradients in the same way as positive gradients. The  $i$ -th client updates its local model on the local dataset  $\mathcal{D}_i$ , and then quantifies and encodes local gradients  $\Delta \mathbf{w}_i$ . Finally, each client sends its encoded gradients  $\mathbf{g}_i$  to the server. The server collects all encoded gradients from clients and aggregates them directly in an encoded domain. Then, the server decodes gradients  $\mathbf{g}_{rec}$  which is reconstructed from aggregated gradients. In our experiments, the sizes of  $\mathbf{g}^+$  and  $\mathbf{g}^-$  are all set to  $\frac{d}{2}$ . Therefore, FedAGE brings no additional communication burden except a slight calculation overhead due to the encoder-decoder network.

### 3.4. Mathematical Analysis

In this part, we analyze the mathematical properties of FedAGE. First of all, our analyses are based on the empirical observation about the encoding-decoding errors (see Appendix F.2). It demonstrates that the encoding-decoding

---

#### Algorithm 1 FedAvg with encoded gradients aggregation

---

**Input:** Initial model  $\mathbf{w}^0$ , well-pretrained autocoders  $(E_c, D_c)$ , communication round  $T$ , client set  $C$ , learning rate  $\eta$ , client dataset  $\mathcal{D}$ , quantization level  $s$  and quantization function  $Q(\cdot; s, n)$ .

**function** ServerProcedure:

**for**  $t \in [T]$  **do**

    choose a subset of client  $C^t \subseteq C, m = |C^t|$

**for**  $i \in C^t$  **in parallel do**

$\mathbf{g}_i^+, \mathbf{g}_i^- \leftarrow \text{ClientUpdate}(\mathbf{w}^t, s, n)$

**end for**

$\mathbf{g}^+ \leftarrow \frac{1}{m} \sum_{i \in C^t} \mathbf{g}_i^+$

$\mathbf{g}^- \leftarrow \frac{1}{m} \sum_{i \in C^t} \mathbf{g}_i^-$

$\mathbf{g}_{rec} \leftarrow \frac{n}{s} (D_c(\mathbf{g}^+) - D_c(\mathbf{g}^-))$

    /\* replaceable \*/

$\mathbf{w}^{t+1} \leftarrow \mathbf{w}^t + \eta \mathbf{g}_{rec}$

**end for**

**end function**

**function** ClientUpdate( $\mathbf{w}^t, s, n$ ):

$\mathbf{w} \leftarrow \mathbf{w}^t$

    /\* replaceable \*/

**for**  $k$  epochs **do**

$\mathbf{w} \leftarrow \mathbf{w} - \eta \nabla f_i(\mathbf{w}; \mathcal{D}_i)$

**end for**

$\Delta \mathbf{w} \leftarrow (\mathbf{w} - \mathbf{w}^t) / \eta$

$\Delta \mathbf{w}^+, \Delta \mathbf{w}^- \leftarrow \text{Max}(\Delta \mathbf{w}, \mathbf{0}), \text{Min}(\Delta \mathbf{w}, \mathbf{0})$

$\mathbf{g}^- \leftarrow E_c(Q(-\Delta \mathbf{w}^- \cdot \lambda_i, s, n))$

$\mathbf{g}^+ \leftarrow E_c(Q(\Delta \mathbf{w}^+ \cdot \lambda_i, s, n))$

    return  $\mathbf{g}^+, \mathbf{g}^-$

**end function**

---

errors  $\nu$  (defined in Equation (8)) can be regarded as a random Gaussian noise (i.e.,  $\nu \sim \mathcal{N}(0, \sigma_\nu^2 \mathbf{I})$ ). The  $\sigma_\nu$  denotes the standard variance of  $\nu$ . Therefore, we rewrite Equation (8) as:

$$D_c \left( \frac{1}{m} \sum_{i=1}^m E_c(\mathbf{l}_i) \right) = \frac{1}{m} \sum_{i=1}^m \mathbf{l}_i + \nu. \quad (9)$$

From this equation, we can see that FedAGE introduces a random noise to aggregation results in the quantization domain.

**Bound of Errors.** Here we discuss the impacts of the noise  $\nu$  on gradients. Firstly, we present Lemma 3.1, which indicates the variance bound of quantization strategy. The proof is described in Appendix B.1.

**Lemma 3.1.** *The variance of the  $k$ -th quantified gradients aggregation  $\left\| \frac{n}{s} \frac{1}{m} \sum_{i=1}^m Q(\mathbf{x}_i^k, s, n) - \frac{1}{m} \sum_{i=1}^m \mathbf{x}_i^k \right\|_2^2$  is bounded by  $\frac{n}{m} \min(\frac{d}{s^2}, \frac{\sqrt{d}}{s})$ .*

Our framework adds an extra random Gaussian noise  $\nu$

to the results in the quantization domain  $Q_s^d$ . Therefore, we study its impacts and present the variance bound of FedAGE in Theorem 3.2. The proof of Theorem 3.2 is shown in Appendix B.2.

**Theorem 3.2.** *The variance of  $k$ -th encoded gradients aggregation  $\|\frac{n}{s}D_c(\frac{1}{m}\sum_{i=1}^m E_c(Q(\mathbf{x}_i^k; s, n))) - \frac{1}{m}\sum_{i=1}^m \mathbf{x}_i^k\|_2^2$  is bounded by  $\frac{n}{m}\min(\frac{d}{s^2}, \frac{\sqrt{d}}{s}) + \frac{n^2}{s^2} \cdot \sigma_\nu^2$ .*

Theorem 3.2 demonstrates that the encoding-decoding errors are bounded. Furthermore, the variance bound can be adjusted by changing normalization parameter  $n$ , quantization level  $s$  and the number of clients  $m$ . In other words, we can increase  $m$ ,  $s$  and reduce  $n$  for the lower magnitude of the noise. The further empirical study about  $m$ ,  $s$ ,  $n$  is presented in Appendix F.2.

**Differential Privacy.** As FedAGE adds a Gaussian noise to the outputs, we prove that FedAGE is a Gaussian mechanism for  $(\epsilon, \delta)$ -DP (Dwork & Roth, 2014). We have  $D_c(\sum_{i=1}^m E_c(\mathbf{l}_i)) = q(\sum_{i=1}^m \mathbf{l}_i) + \nu$ , where the real-valued query function  $q(\sum_{i=1}^m \mathbf{l}_i) = \sum_{i=1}^m \mathbf{l}_i$ . Therefore, FedAGE is a Gaussian mechanism for  $(\epsilon, \delta)$ -DP according to the definition of Gaussian mechanism, which is summarised in Appendix C.2. We describe the sensitivity of query function  $q$  in Corollary 3.3, which is proved in Appendix B.3.

**Corollary 3.3.** *For adjacent FL datasets  $\mathcal{D}$  and  $\mathcal{D}'$ , the query function  $q$  denotes the aggregated gradients. The sensitivity of the query function in FedAGE is given by*

$$\Delta q = \max_{\text{adjacent } \mathcal{D}, \mathcal{D}'} \|q(\mathbf{l}^{\mathcal{D}}) - q(\mathbf{l}^{\mathcal{D}'})\| = \frac{s}{m}.$$

The original noise  $\nu$  is added to the quantization domain. Therefore, the noise in the real domain can be adjusted by  $n$ . Formally, the relation between the standard variance of  $\sigma_\nu$  and DP level  $(\epsilon, \delta)$  is given by  $n\sigma_\nu \geq \frac{\sqrt{2 \ln(1.25/\delta)}}{\epsilon} \frac{s^2}{m}$ . In this inequality, both quantization level  $s$  and noise variance  $\sigma_\nu$  depend on encoder-decoder, while the client number  $m$  is set beforehand. Therefore, we can change the normalization parameter  $n$  dynamically to achieve different DP levels  $(\epsilon, \delta)$  over the training process. The empirical study about DP level of FedAGE is presented in Section 4.2.

**Convergence Analysis.** Here we analyze the convergence performance of FedAGE. Given access to stochastic gradients, and a starting point  $\mathbf{w}^0$ , build iterates  $\mathbf{w}^t$  given by Algorithm 1. In this setting, we have:

**Theorem 3.4.** *Let  $\mathcal{W} \subseteq \mathbb{R}^d$  be convex, and let  $f : \mathcal{W} \rightarrow \mathbb{R}$  be unknown,  $\mu$ -strongly convex, and  $L$ -smooth. Let the variance of the stochastic gradient in each clients is upper bounded  $\mathbb{E}[\|\nabla f_i(\mathbf{w})\|_2^2] \leq G^2$ . Let  $\mathbf{w}^0 \in \mathcal{W}$  be given, and let  $R^2 = \sup_{\mathbf{w} \in \mathcal{W}} \|\mathbf{w} - \mathbf{w}^0\|^2$ . Let  $T > 0$  be fixed.*

Considering  $\eta_t = \eta \leq \min\{1, \frac{1}{\mu k}\}$  and  $k = 1$ , we have

$$\begin{aligned} \mathbb{E}[f(\mathbf{w}^T)] - \min_{\mathbf{w} \in \mathcal{W}} f(\mathbf{w}) &\leq \frac{L}{2}(1 - \mu\eta)^T R^2 \\ &+ \frac{\eta L}{2\mu} \left( G^2 + \frac{n^2}{s^2} d\sigma_\nu^2 \right) (1 - (1 - \mu\eta)^T). \end{aligned}$$

Theorem 3.4 is convergence analysis results when  $k = 1$  (i.e., each client performs once gradient descent locally). For more general conclusions, please see our proof in Appendix D. Theorem 3.4 demonstrates the factors of affecting the optimization performance of FedAGE. It suggests choosing a larger quantization level  $s$  and well-pretrained encoder-decoder with lower  $\sigma_\nu$ . The normalization parameter  $n$  is supposed to dynamically decay over the training process for better convergence results.

## 4. Experiment Evaluation

In this section, we evaluate FedAGE on different tasks: image classification on MNIST (Deng, 2012) and CIFAR-10 (Krizhevsky et al., 2009), next-word-prediction on Shakespeare (Shakespeare, 2014; Caldas et al., 2018). The details of FL experiment settings are summarized in Appendix F.

**Network Architecture.** We define two different convolutional neural networks (CNN) for MNIST and CIFAR-10 datasets, and a recurrent neural network (RNN) for Shakespeare dataset. The architectures of CNN are depicted in Table 2. For the next-world-prediction task, we embed each character into a learned 8-dimensional space. The RNN model consists of two LSTM layers with 256 units and a final softmax output layer with one unit per character.

**Federated Data Partition.** For the MNIST dataset, we randomly split the training data samples into 100 subsets equally which is referred to as IID data partition. For Non-IID data partition, we sort the dataset samples by labels and split them into 200 shards. Then, we assign two shards to each different client (McMahan et al., 2017). We randomly partition CIFAR-10 dataset into 10 clients to evaluate the performance in a cross-silo setting. For the Shakespeare dataset, we follow LEAF (Caldas et al., 2018), which partitions Shakespeare into 660 clients. The number of data samples is different among clients. Therefore, we refer to this setting as unbalanced (i.e., Non-IID).

We pretrain three encoder-decoder networks for the number of clients  $m = 5, 10, 40$  with the same quantization level  $s = 64$ . Each encoder-decoder pair corresponds with a task for all training hyper-parameters in this paper, which reveals the adaptability of FedAGE. Full details of the pretraining procedure are presented in Appendix F.2.

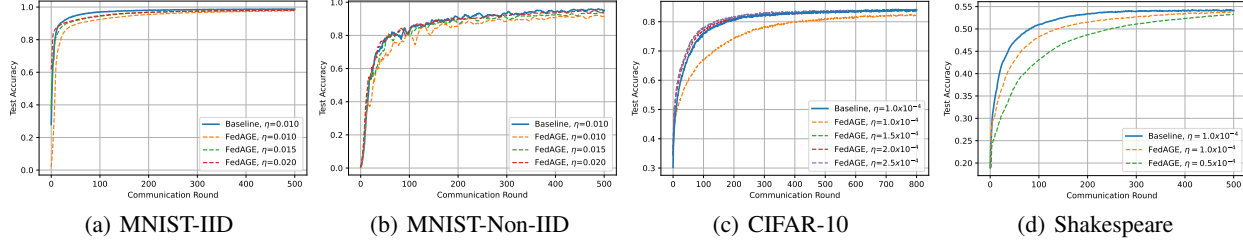


Figure 2. Convergence performance of FedAGE. FedAGE learns slower than FedAvg under the same learning rate. As FedAGE adds random noise to gradients for protection, subdued convergence curve is acceptable. By increasing learning rate slightly, we can mitigate the phenomenons.

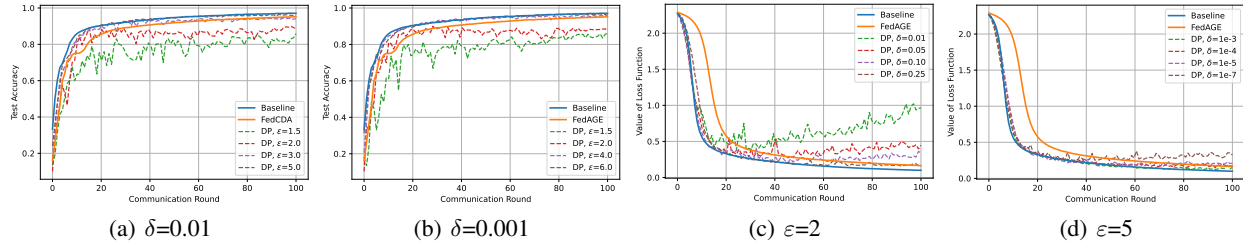


Figure 3. Estimate the DP level ( $\delta, \epsilon$ ) of noise  $\nu$ . To the best of our knowledge, the convergence curve changes continuously with the change of DP parameters. Therefore, we estimate the DP level of FedAGE by investigating where its convergence curve lays.

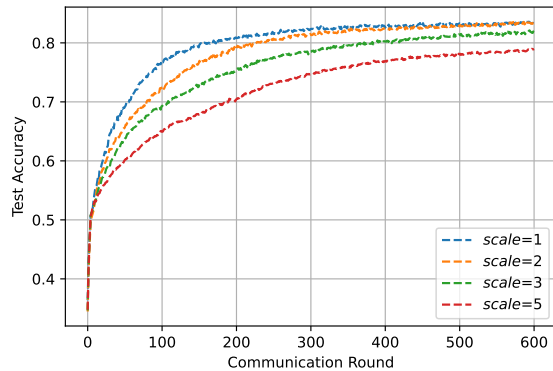


Figure 4. The impact of  $n$  on convergence performance. The parameter  $scale$  indicates the magnification of  $n$  over the FL process. The higher  $n$  brings the larger magnitude of noise, leading to slower convergence.

#### 4.1. Convergence Performance

In this part, we study the impact of FedAGE on FL convergence. We take FedAvg with a fixed learning rate as baseline federated optimization algorithm. To achieve better convergence results according to Theorem 3.4, we dynamically set  $n$  as the largest absolute value of gradients in each round. Typically,  $n$  decays over the process of training.

The convergence performance of FedAGE is shown in Figure 2. The results reveal that FedAGE is slightly slower

than FedAvg under the same  $\eta$ , which is expected in the previous analysis. Importantly, FedAGE does not damage the performance of final model in all three tasks.

#### 4.2. Differential Privacy Level

FedAGE is proved to be a Gaussian mechanism for  $(\epsilon, \delta)$ -DP. Here we estimate the DP level of FedAGE. In previous analysis, the DP level of FedAGE corresponds to the value of  $n$ . However,  $n$  is changing over FL training process in our practice. Therefore, to estimate the overall DP level of FedAGE, we compare our framework with the DPSGD (Wei et al., 2020; Abadi et al., 2016) on the MNIST data.

The details of DPSGD are summarised in Appendix C. We set the norm gradient clipping bound  $B = 20$ . Then we fix the standard variance of DP Gaussian noise as  $\sigma = \frac{\sqrt{2 \ln(1.25/\delta)} B}{\epsilon}$ . In DPSGD,  $(\delta, \epsilon)$  is hyper-parameters of DP corresponding with the magnitude of DP Gaussian noise.

Firstly, we fix different privacy budget  $\epsilon = 2, 5$  to estimate the relaxation term  $\delta$  of noise  $\nu$ . Then, we fix relaxation term  $\delta = 0.01, 0.001$  to estimate the privacy budget  $\epsilon$  of noise  $\nu$ . Experiment results are shown in Figure 3.

For further discussion, FedAGE supports adjusting the magnitude of gradient by changing normalization parameters  $n$ , as the standard variance of real-value Gaussian noise  $\sigma = \frac{n}{s} \sigma_\nu$  corresponds with  $n$ . Then, We empirically study

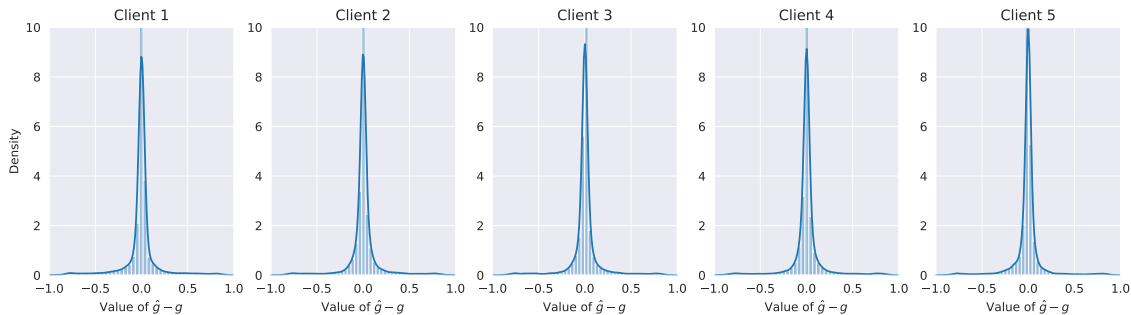


Figure 5. The differences between differential attack results and ground-truth gradients of clients.

Table 1. The visualization of gradient inversion procedure. We perform DLG (Zhao et al., 2020) on raw gradients and the gradients obtained by differential attack respectively. The left column indicates the iteration epoch of DLG.

Iter	Raw	Ours	Raw	Ours
0				
20				
40				
80				
120				

its impact on convergence performance. The results are shown in Figure 4.

### 4.3. Gradient Protection Ability

In this part, we evaluate the protection ability of FedAGE on a vulnerable setting (i.e., easy to be attacked). Firstly, we construct differential attack from the perspective of the FL server, trying to steal raw gradients from encoded gradients under FedAGE framework. Then, we try to restore data points from the gradients via gradient inversion methods DLG (Zhao et al., 2020). The experiment setting of this part follows DLG, in which the base model is LeNet-5 (LeCun et al., 2015), and the activation function of LeNet-5 is the sigmoid.

A server can try to obtain raw gradients through differential attack. The attack procedure is described as follows: (1) the server decodes the aggregated gradients  $g$ ; (2) it replaces

encoded gradients of the  $i$ -th client with  $E_c(\mathbf{0})$ , and then decodes the results  $\bar{g}_i$ ; and (3) server makes difference to obtain gradients of the  $i$ -th client by  $\hat{g}_i = g - \bar{g}_i$ .

In our experiment, five clients perform one step of gradient descent with a single data point respectively, which is the most vulnerable setting. Each client uploads its encoded gradients denoted by  $g_1, \dots, g_5$ . Then we perform the differential attack to obtain all five gradients  $\hat{g}_1, \dots, \hat{g}_5$  respectively. For all  $i \in [1, 5]$ , we observe the difference between  $\hat{g}_i$  and  $g_i$ . The probability density curves of the difference are depicted in Figure 5. Then, we perform the DLG procedure on the gradients obtained by differential attack respectively. The visualization of gradient inversion procedure is shown in Table 1 (full results are in Appendix F.3). DLG suggests that sufficient large magnitude of noise prevents deep leakage. Therefore, our experiments results indicate that the noise of FedAGE is sufficient enough to defend against differential attack.

## 5. Conclusion

In this work, we propose a practical framework FedAGE, which enables gradients to be aggregated in an encoded domain to protect the privacy of gradients. Furthermore, we theoretically prove that the corresponding algorithm has convergence guarantee and the encoding-decoding errors are bounded. Also, FedAGE is a Gaussian mechanism for differential privacy. Our empirical results demonstrate that FedAGE is adaptive to different FL settings while maintaining the final performance of FL models. The gradient protection study also shows that FedAGE is capable of preventing gradients leakage.

## References

- Abadi, M., Chu, A., Goodfellow, I., McMahan, H. B., Mironov, I., Talwar, K., and Zhang, L. Deep learning with differential privacy. In *Proceedings of the 2016 ACM SIGSAC conference on computer and communications security*, pp. 308–318, 2016.



- Abrahamyan, L., Chen, Y., Bekoulis, G., and Deligiannis, N. Learned gradient compression for distributed deep learning. *CoRR*, abs/2103.08870, 2021.
- Alistarh, D., Grubic, D., Li, J., Tomioka, R., and Vojnovic, M. Qsgd: Communication-efficient sgd via gradient quantization and encoding. *Advances in Neural Information Processing Systems*, 30:1709–1720, 2017.
- Amiri, M. M., Gunduz, D., Kulkarni, S. R., and Poor, H. V. Federated learning with quantized global model updates. *arXiv preprint arXiv:2006.10672*, 2020.
- Basu, D., Data, D., Karakus, C., and Diggavi, S. N. Qsparse-local-sgd: Distributed SGD with quantization, sparsification, and local computations. *IEEE J. Sel. Areas Inf. Theory*, 1(1):217–226, 2020. doi: 10.1109/jsait.2020.2985917.
- Bhagoji, A. N., Chakraborty, S., Mittal, P., and Calo, S. B. Analyzing federated learning through an adversarial lens. In Chaudhuri, K. and Salakhutdinov, R. (eds.), *Proceedings of the 36th International Conference on Machine Learning, ICML 2019, 9-15 June 2019, Long Beach, California, USA*, volume 97 of *Proceedings of Machine Learning Research*, pp. 634–643. PMLR, 2019.
- Caldas, S., Wu, P., Li, T., Konečný, J., McMahan, H. B., Smith, V., and Talwalkar, A. LEAF: A benchmark for federated settings. *CoRR*, abs/1812.01097, 2018.
- Cormode, G., Jha, S., Kulkarni, T., Li, N., Srivastava, D., and Wang, T. Privacy at scale: Local differential privacy in practice. In *Proceedings of the 2018 International Conference on Management of Data*, pp. 1655–1658, 2018.
- Deng, L. The mnist database of handwritten digit images for machine learning research [best of the web]. *IEEE Signal Processing Magazine*, 29(6):141–142, 2012.
- Dwork, C. and Roth, A. The algorithmic foundations of differential privacy. *Found. Trends Theor. Comput. Sci.*, 9(3-4):211–407, 2014.
- Gentry, C. Fully homomorphic encryption using ideal lattices. In *Proceedings of the forty-first annual ACM symposium on Theory of computing*, pp. 169–178, 2009.
- He, K., Zhang, X., Ren, S., and Sun, J. Deep residual learning for image recognition. In *Proceedings of the IEEE conference on computer vision and pattern recognition*, pp. 770–778, 2016.
- Kairouz, P., McMahan, H. B., Avent, B., Bellet, A., Bennis, M., Bhagoji, A. N., Bonawitz, K., Charles, Z., Cormode, G., Cummings, R., et al. Advances and open problems in federated learning. *arXiv preprint arXiv:1912.04977*, 2019.
- Krizhevsky, A., Hinton, G., et al. Learning multiple layers of features from tiny images. 2009.
- LeCun, Y. et al. Lenet-5, convolutional neural networks. URL: <http://yann.lecun.com/exdb/lenet>, 20(5):14, 2015.
- Li, H. and Han, T. An end-to-end encrypted neural network for gradient updates transmission in federated learning. In *DCC*, pp. 589. IEEE, 2019.
- Li, T., Sahu, A. K., Zaheer, M., Sanjabi, M., Talwalkar, A., and Smith, V. Federated optimization in heterogeneous networks. In *MLSys*. mlsys.org, 2020a.
- Li, T., Sanjabi, M., Beirami, A., and Smith, V. Fair resource allocation in federated learning. In *ICLR*. OpenReview.net, 2020b.
- Lin, Y., Han, S., Mao, H., Wang, Y., and Dally, B. Deep gradient compression: Reducing the communication bandwidth for distributed training. In *6th International Conference on Learning Representations, ICLR 2018, Vancouver, BC, Canada, April 30 - May 3, 2018, Conference Track Proceedings*. OpenReview.net, 2018.
- McMahan, B., Moore, E., Ramage, D., Hampson, S., and y Arcas, B. A. Communication-efficient learning of deep networks from decentralized data. In Singh, A. and Zhu, X. J. (eds.), *Proceedings of the 20th International Conference on Artificial Intelligence and Statistics, AISTATS 2017, 20-22 April 2017, Fort Lauderdale, FL, USA*, volume 54 of *Proceedings of Machine Learning Research*, pp. 1273–1282. PMLR, 2017.
- Paillier, P. Public-key cryptosystems based on composite degree residuosity classes. In *International conference on the theory and applications of cryptographic techniques*, pp. 223–238. Springer, 1999.
- Seide, F., Fu, H., Droppo, J., Li, G., and Yu, D. 1-bit stochastic gradient descent and its application to data-parallel distributed training of speech dnns. In *INTERSPEECH*, pp. 1058–1062. ISCA, 2014.
- Shakespeare, W. *The complete works of William Shakespeare*. Race Point Publishing, 2014.
- Shi, S., Chu, X., Cheung, K. C., and See, S. Understanding top-k sparsification in distributed deep learning. *arXiv preprint arXiv:1911.08772*, 2019.
- Simonyan, K. and Zisserman, A. Very deep convolutional networks for large-scale image recognition. In *ICLR*, 2015.
- Triastcyn, A. and Faltings, B. Federated learning with bayesian differential privacy. In *IEEE BigData*, pp. 2587–2596. IEEE, 2019.

- Truex, S., Liu, L., Chow, K. H., Gursoy, M. E., and Wei, W. Ldp-fed: federated learning with local differential privacy. In *EdgeSys@EuroSys*, pp. 61–66. ACM, 2020.
- Wei, K., Li, J., Ding, M., Ma, C., Yang, H. H., Farokhi, F., Jin, S., Quek, T. Q. S., and Poor, H. V. Federated learning with differential privacy: Algorithms and performance analysis. *IEEE Trans. Inf. Forensics Secur.*, 15:3454–3469, 2020.
- Yang, Q., Liu, Y., Chen, T., and Tong, Y. Federated machine learning: Concept and applications. *ACM Trans. Intell. Syst. Technol.*, 10(2):12:1–12:19, 2019.
- Yao, A. C.-C. How to generate and exchange secrets. In *27th Annual Symposium on Foundations of Computer Science (sfcs 1986)*, pp. 162–167, 1986. doi: 10.1109/SFCS.1986.25.
- Yin, H., Mallya, A., Vahdat, A., Alvarez, J. M., Kautz, J., and Molchanov, P. See through gradients: Image batch recovery via gradinversion. In *IEEE Conference on Computer Vision and Pattern Recognition, CVPR 2021, virtual, June 19-25, 2021*, pp. 16337–16346. Computer Vision Foundation / IEEE, 2021.
- Zhang, C., Li, S., Xia, J., Wang, W., Yan, F., and Liu, Y. Batchcrypt: Efficient homomorphic encryption for cross-silo federated learning. In Gavrilovska, A. and Zadok, E. (eds.), *2020 USENIX Annual Technical Conference, USENIX ATC 2020, July 15-17, 2020*, pp. 493–506. USENIX Association, 2020.
- Zhao, B., Mopuri, K. R., and Bilen, H. idlg: Improved deep leakage from gradients. *CoRR*, abs/2001.02610, 2020.
- Zhu, L. and Han, S. Deep leakage from gradients. In *Federated Learning*, volume 12500 of *Lecture Notes in Computer Science*, pp. 17–31. Springer, 2020.

## Supplementary Material

We provide details omitted in the main paper.

- Appendix A : details of stochastic quantization.
- Appendix B : additional proofs of lemma, theorem and corollary.
- Appendix C : additional materials about differential privacy.
- Appendix D : details of convergence analysis.
- Appendix F : details of experimental setups and implementations.

### A. Stochastic Quantization

Let  $\mathbf{x} \in \mathbb{R}^d$ , with the  $k$ -th element denoted by  $x^k$ . Given a quantization level  $s \geq 1$ , we have

$$Q(\mathbf{x}^k, n, s) \triangleq \text{sign}(\mathbf{x}^k) \cdot n \cdot \xi(\mathbf{x}^k, s), \quad (10)$$

where  $\xi(\mathbf{x}^k, s)$  are independent random variables defined as follows. We highlight that the sign of  $x^k$  is positive in this paper. Therefore,  $\text{sign}(\mathbf{x}^k) \equiv 1$ . Furthermore, the normalization parameter  $n$  is set beforehand, rather than  $n = \|\mathbf{x}\|_2$  or  $\|\mathbf{x}\|_\infty$  as QSGD (Alistarh et al., 2017) proposed.

$$\xi(\mathbf{x}^k, s) \triangleq \begin{cases} l/s, & \text{with probability } 1 - (\frac{\mathbf{x}^k}{n} s - l), \\ (l+1)/s & \text{otherwise.} \end{cases} \quad (11)$$

In all, we define quantization function  $Q(\mathbf{x}, s, n) \triangleq \mathbf{l}$  in our work, where  $0 \leq \mathbf{l}^k \leq s$  is a stochastic integer corresponding with the real-value  $\mathbf{x}^k$ .

### B. Proofs

#### B.1. Proof of Lemma 3.1

*Proof.* We assume  $\mathbf{x} \in \mathbb{R}^d$ ,  $0 \leq k < d$ . For all  $k$ -th element of vectors  $(\mathbf{x}_1, \mathbf{x}_2, \dots, \mathbf{x}_m)$ . The variance bound of quantified vector is given by:

$$\begin{aligned} & \mathbb{E}(\| \frac{n}{s} \frac{1}{m} \sum_{i=1}^m Q(\mathbf{x}_i^k, s, n) - \frac{1}{m} \sum_{i=1}^m \mathbf{x}_i^k \|_2^2) \\ &= \frac{1}{m^2} \mathbb{E}(\| \sum_{i=1}^m (\frac{n}{s} Q(\mathbf{x}_i^k, s, n) - \mathbf{x}_i^k) \|_2^2) \\ &\leq \frac{1}{m^2} \mathbb{E}(\sum_{i=1}^m \| \frac{n}{s} \mathbf{l}_i^k - \mathbf{x}_i^k \|_2^2) \quad (\text{by lemma 3.1 (Alistarh et al., 2017)}) \\ &\leq \frac{n}{m^2} \sum_{i=1}^m \min(\frac{d}{s^2}, \frac{\sqrt{d}}{s}) \\ &= \frac{n}{m} \min(\frac{d}{s^2}, \frac{\sqrt{d}}{s}). \end{aligned}$$

□

## B.2. Proof of Theorem 3.2

*Proof.* We assume  $\mathbf{x} \in \mathbb{R}^d$ ,  $0 \leq k < d$ . For all  $k$ -th element of vectors  $(\mathbf{x}_1, \mathbf{x}_2, \dots, \mathbf{x}_m)$ . If noise  $\boldsymbol{\nu} \sim \mathcal{N}(0, \sigma_\nu^2 \mathbf{I})$ , then we have the variance bound of FedAGE:

$$\begin{aligned}
 & \mathbb{E} \left( \left\| \frac{n}{s} D_c \left( \frac{1}{m} \sum_{i=1}^m E_c(Q(\mathbf{x}_i^k, s, n)) \right) - \frac{1}{m} \sum_{i=1}^m \mathbf{x}_i^k \right\|_2^2 \right) \\
 &= \mathbb{E} \left( \left\| \frac{n}{s} \left( \frac{1}{m} \sum_{i=1}^m \mathbf{l}_i^k + \boldsymbol{\nu}^k \right) - \frac{1}{m} \sum_{i=1}^m \mathbf{x}_i^k \right\|_2^2 \right) \quad (\text{by Equation 9}) \\
 &= \mathbb{E} \left( \left\| \frac{1}{m} \sum_{i=1}^m \frac{n}{s} \mathbf{l}_i^k - \frac{1}{m} \sum_{i=1}^m \mathbf{x}_i^k + \frac{n}{s} \boldsymbol{\nu}^k \right\|_2^2 \right) \\
 &\leq \mathbb{E} \left( \left\| \frac{1}{m} \sum_{i=1}^m \frac{n}{s} \mathbf{l}_i^k - \frac{1}{m} \sum_{i=1}^m \mathbf{x}_i^k \right\|_2^2 \right) + \mathbb{E} \left( \left\| \frac{n}{s} \boldsymbol{\nu}^k \right\|_2^2 \right) \\
 &\leq \mathbb{E} \left( \left\| \frac{1}{m} \sum_{i=1}^m \frac{n}{s} \mathbf{l}_i^k - \frac{1}{m} \sum_{i=1}^m \mathbf{x}_i^k \right\|_2^2 \right) + \frac{n^2}{s^2} \mathbb{E} \left( \left\| \boldsymbol{\nu}^k \right\|_2^2 \right) \\
 &\leq \frac{1}{m^2} \mathbb{E} \left( \sum_{i=1}^m \left\| \frac{n}{s} \mathbf{l}_i^k - \mathbf{x}_i^k \right\|_2^2 \right) + \frac{n^2}{s^2} \mathbb{E} \left( \left\| \boldsymbol{\nu}^k \right\|_2^2 \right) \quad (\text{by lemma 3.1}) \\
 &\leq \frac{n}{m} \min \left( \frac{d}{s^2}, \frac{\sqrt{d}}{s} \right) + \frac{n^2}{s^2} \sigma_\nu^2.
 \end{aligned}$$

□

## B.3. Proof of Corollary 3.3

*Proof.* The sensitivity of query  $q$  can be defined as:

$$\Delta q = \max_{\text{adjacent } \mathcal{D}, \mathcal{D}'} \left\| q(\mathbf{l}^{\mathcal{D}}) - q(\mathbf{l}^{\mathcal{D}'}) \right\|, \quad (12)$$

where  $\mathcal{D}$  is the overall dataset in FL system and  $\mathbf{l}^{\mathcal{D}}$  indicates the quantified gradients on  $\mathcal{D}$ . Based on FedAGE scheme, we have

$$q(\mathbf{l}^{\mathcal{D}}) = \frac{1}{m} [\mathbf{l}_1^{\mathcal{D}_1} + \dots + \mathbf{l}_i^{\mathcal{D}_i} + \dots + \mathbf{l}_m^{\mathcal{D}_m}], \quad (13)$$

and

$$q(\mathbf{l}^{\mathcal{D}'}) = \frac{1}{m} [\mathbf{l}_1^{\mathcal{D}'_1} + \dots + \mathbf{l}_i^{\mathcal{D}'_i} + \dots + \mathbf{l}_m^{\mathcal{D}'_m}], \quad (14)$$

where  $\mathcal{D} = \mathcal{D}_1 \cup \dots \cup \mathcal{D}_m$  and  $\mathbf{l}_i^{\mathcal{D}_i}$  indicates the quantified gradient of the  $i$ -th client. Therefore, the sensitivity can be given by

$$\begin{aligned}
 \Delta q &= \max_{\text{adjacent } \mathcal{D}, \mathcal{D}'} \left\| q(\mathbf{l}^{\mathcal{D}}) - q(\mathbf{l}^{\mathcal{D}'}) \right\| \\
 &= \frac{1}{m} \max_{\text{adjacent } \mathcal{D}, \mathcal{D}'} \left\| \mathbf{l}_i^{\mathcal{D}_i} - \mathbf{l}_i^{\mathcal{D}'_i} \right\| = \frac{s}{m}.
 \end{aligned} \quad (15)$$

□

## C. Differential Privacy

### C.1. The Gaussian Mechanism for Differential Privacy

**Definition C.1. Differential Privacy (Dwork & Roth, 2014):** A randomized mechanism  $\mathcal{M} : \mathcal{D} \rightarrow \mathcal{R}$  with domain  $\mathcal{D}$  and range  $\mathcal{R}$  satisfies  $(\epsilon, \delta)$ -differentially private, if for any two adjacent databases  $d, d' \in \mathcal{D}$  and for any subset of outputs  $\mathcal{S} \subseteq \mathcal{R}$  is holds that

$$Pr[\mathcal{M}(d) \in \mathcal{S}] \leq e^\epsilon Pr[\mathcal{M}(d') \in \mathcal{S}] + \delta.$$

**Theorem C.2. The Gaussian Mechanism** (Dwork & Roth, 2014): Let  $q : \mathbb{N}^{|\mathcal{X}|} \rightarrow \mathbb{R}^d$  be an arbitrary  $d$ -dimensional function, and define its  $l_2$  sensitivity to be  $\Delta_2 q = \max_{\text{adjacent } D, D'} \|q(D) - q(D')\|$ . The Gaussian mechanism with parameter  $\sigma$  adds noise scaled to  $\mathcal{N}(0, \sigma^2)$  to each of the  $d$  components of the output. Let  $\varepsilon \in (0, 1)$  be arbitrary. For  $c^2 > 2 \ln(1.25/\delta)$ , the Gaussian mechanism  $M$  with parameter  $\sigma \geq c\Delta_2 f/\varepsilon$  is  $(\varepsilon, \delta)$ -differentially private.

$$M(D) = q(D) + \nu, \text{ where } \nu \sim \mathcal{N}(0, \sigma^2).$$

## C.2. Differential Privacy SGD

We summarise our implementation about DPSGD in Algorithm 2.

---

### Algorithm 2 Defferential Privacy SGD on FedAvg

---

**Input:** Initial model  $\mathbf{w}^0$ , client set  $C$ , client dataset  $\mathcal{D}$ , gradient norm bound  $B$ , communication round  $T$ , learning rate  $\eta$ .

**function** ServerProcedure:

**for**  $t = 0$  **to**  $T$  **do**

**choose a subset of client**  $C^t \subseteq C, m = |C^t|$

**for**  $i \in C^t$  **in parallel do**

$\Delta \hat{\mathbf{w}}_i \leftarrow \text{ClientUpdate}(\mathbf{w}^t)$

**end for**

**Add noise**

$\hat{\mathbf{g}} \leftarrow \frac{1}{m} \sum_{i \in C^t} \Delta \hat{\mathbf{w}}_i + \mathcal{N}(0, \sigma^2 B^2 \mathbf{I})$

$\mathbf{w}^{t+1} \leftarrow \mathbf{w}^t - \eta \hat{\mathbf{g}}$

**end for**

**end function**

**function** ClientUpdate( $\mathbf{w}^t$ ):

$\mathbf{w} \leftarrow \mathbf{w}^t$

**for**  $k$  epochs **do**

$\mathbf{w} \leftarrow \mathbf{w} - \eta \nabla f_i(\mathbf{w}; \mathcal{D}_i)$

**end for**

$\Delta \mathbf{w} = (\mathbf{w}^t - \mathbf{w})/\eta$

$\Delta \hat{\mathbf{w}} = \Delta \mathbf{w} / \max(1, \frac{\|\Delta \mathbf{w}\|_2}{B})$

  return  $\Delta \hat{\mathbf{w}}$

**end function**

---

## D. Convergence Analysis

### D.1. Preliminaries

We denote the optimal solution minimizing loss function  $f(\mathbf{w})$  by  $\mathbf{w}^*$ , and the minimum loss as  $f^*$ , i.e.,  $w^* \triangleq \arg \min_{\mathbf{w}} f(\mathbf{w})$ , and  $f^* \triangleq f(\mathbf{w}^*)$ . And the ServerProcedure updates the global model as

$$\mathbf{w}^{t+1} = \mathbf{w}^t - \eta_t \frac{n}{s} \frac{1}{m} D_c \left( \sum_{i=1}^m E_c \left( \sum_{j=1}^k Q(\nabla f_i(\mathbf{w}_{i,j}^t, \xi_{i,j}^t, s, n)) \right) \right) \quad (16)$$

$$= \mathbf{w}^t - \eta_t \frac{1}{m} \sum_{i=1}^m \sum_{j=1}^k \nabla f_i(\mathbf{w}_{i,j}^t, \xi_{i,j}^t) - \eta_t \frac{n}{s} \nu \quad (17)$$

$$= \mathbf{w}^t - \frac{1}{m} \sum_{i=1}^m \Delta \mathbf{w}_i^t - \eta_t \frac{n}{s} \nu. \quad (18)$$

**Assumption D.1** (Smoothness). The loss functions  $f_1, \dots, f_i$  are  $L$ -smooth; that is,  $\forall \mathbf{v}, \mathbf{u} \in \mathbb{R}^d$ ,

$$2(f_i(\mathbf{v}) - f_i(\mathbf{u})) \leq 2\langle \mathbf{v} - \mathbf{u}, \nabla f_i(\mathbf{u}) \rangle + L\|\mathbf{v} - \mathbf{u}\|_2^2, \quad \forall i \in [m]. \quad (19)$$

**Assumption D.2** (Strongly convex). The loss functions  $f_1, \dots, f_i$  are  $\mu$ -strongly convex; that is,  $\forall \mathbf{v}, \mathbf{u} \in \mathbb{R}^d$ ,

$$2(f_i(\mathbf{v}) - f_u(\mathbf{u})) \geq 2\langle \mathbf{v} - \mathbf{u}, \nabla f_i(\mathbf{u}) \rangle + \mu \|\mathbf{v} - \mathbf{u}\|_2^2, \quad \forall i \in [m]. \quad (20)$$

**Assumption D.3** (Bounded variance). The expected squared  $l_2$ -norm of the stochastic gradients are bounded, i.e.,

$$\mathbb{E}_\xi \left[ \|\nabla f_i(\mathbf{w}_{i,j}^t, \xi_{i,j}^t)\|_2^2 \right] \leq G^2, \quad \forall i \in [k], \forall i \in [m], \forall t. \quad (21)$$

## D.2. Convergence Rate

**Theorem D.4.** Let  $0 < \eta_t \leq \min \left\{ 1, \frac{1}{\mu k} \right\}, \forall t$ . We have

$$\mathbb{E} \left[ \|\mathbf{w}^t - \mathbf{w}^*\|_2^2 \right] \leq \left( \prod_{i=0}^{t-1} A(i) \right) \|\mathbf{w}(0) - \mathbf{w}^*\|_2^2 + \sum_{i=0}^{t-1} B(i) \prod_{j=i+1}^{t-1} A(j), \quad (22)$$

where

$$A(i) \triangleq 1 - \mu \eta_i (k - \eta_i (k - 1)) \quad (23)$$

$$\begin{aligned} B(i) \triangleq & \eta_t^2 (k^2 + k - 1) G^2 + \eta_t^2 \frac{n^2}{s^2} d \sigma_\nu^2 \\ & + (1 + \mu(1 - \eta_i)) \eta^2(i) G^2 \frac{k(k-1)(2k-1)}{6} + 2\eta_i(k-1)\Gamma. \end{aligned} \quad (24)$$

**Corollary D.5.** From the  $L$ -smoothness of the loss function, for  $0 < \eta_t \leq \min \left\{ 1, \frac{1}{\mu k} \right\}, \forall t$ , and a total of  $T$  global iterations, it follows that

$$\begin{aligned} \mathbb{E}[f(\mathbf{w}^T)] - f^* & \leq \frac{L}{2} \mathbb{E} \left[ \|\mathbf{w}^T - \mathbf{w}^*\|_2^2 \right] \\ & \leq \frac{L}{2} \left( \prod_{i=0}^{T-1} A(i) \right) \|\mathbf{w}^0 - \mathbf{w}^*\|_2^2 + \frac{L}{2} \sum_{j=0}^{T-1} B(j) \prod_{i=j+1}^{T-1} A(i), \end{aligned} \quad (25)$$

where the last inequality follows from (22). Considering  $\eta_t = \eta$  and  $k = 1$ , we have

$$\begin{aligned} \mathbb{E}[f(\mathbf{w}^T)] - f^* & \leq \frac{L}{2} (1 - \mu\eta)^T \|\mathbf{w}^0 - \mathbf{w}^*\|_2^2 \\ & \quad + \frac{\eta L}{2\mu} \left( G^2 + \frac{n^2}{s^2} d \right) (1 - (1 - \mu\eta)^T). \end{aligned} \quad (26)$$

**Asymptotic convergence** Here we show that, for a decreasing learning rate over time, such that  $\lim_{t \rightarrow \infty} \eta_t = 0$ ,  $\lim_{T \rightarrow \infty} \mathbb{E}[f(\mathbf{w}^T)] - f^* = 0$ . For  $0 < \eta_t \leq \min \left\{ 1, \frac{1}{\mu k} \right\}$ , we have  $0 \leq A(t) < 1$ , and  $\lim_{T \rightarrow \infty} \prod_{i=0}^{T-1} A(i) = 0$ . For simplicity, assume  $\eta_t = \frac{\alpha}{t+\beta}$ , for constant values  $\alpha$  and  $\beta$ . For  $j \gg 0$ ,  $B(j) \rightarrow 0$ , and for limited  $j$  values,  $\prod_{i=j+1}^{T-1} A(i) \rightarrow 0$ , and so, according to (12),  $\lim_{T \rightarrow \infty} \mathbb{E}[f(\mathbf{w}^T)] - f^* = 0$ .

## E. Proof of Theorem D.4

*Proof.* We have

$$\begin{aligned} & \mathbb{E} \left[ \|\mathbf{w}^{t+1} - \mathbf{w}^*\|_2^2 \right] \\ & = \mathbb{E} \left[ \|\mathbf{w}^t - \mathbf{w}^*\|_2^2 \right] + \mathbb{E} \left[ \left\| \frac{1}{m} \sum_{i=1}^m \Delta \mathbf{w}_i^t + \eta_t \frac{n}{s} \nu \right\|_2^2 \right] + 2\mathbb{E} \left[ \langle \mathbf{w}^t - \mathbf{w}^*, \frac{1}{m} \sum_{i=1}^m \Delta \mathbf{w}_i^t + \eta_t \nu \rangle \right] \\ & \leq \mathbb{E} \left[ \|\mathbf{w}^t - \mathbf{w}^*\|_2^2 \right] + \mathbb{E} \left[ \left\| \frac{1}{m} \sum_{i=1}^m \Delta \mathbf{w}_i^t \right\|_2^2 \right] + \mathbb{E} \left[ \left\| \eta_t \frac{n}{s} \nu \right\|_2^2 \right] + 2\mathbb{E} \left[ \langle \mathbf{w}^t - \mathbf{w}^*, \frac{1}{m} \sum_{i=1}^m \Delta \mathbf{w}_i^t \rangle \right]. \end{aligned} \quad (27)$$

From the convexity of  $\|\cdot\|_2^2$ , it follows that

$$\begin{aligned}
 \mathbb{E}\left[\left\|\frac{1}{m}\sum_{i=1}^m\Delta\mathbf{w}_i^t\right\|_2^2\right] &\leq\frac{1}{m}\sum_{i=1}^m\mathbb{E}\left[\|\Delta\mathbf{w}_i^t\|_2^2\right] \\
 &=\eta_t^2\frac{1}{m}\sum_{i=1}^m\mathbb{E}\left[\left\|\sum_{j=1}^k\nabla f_i(\mathbf{w}_{i,j}^t,\xi_{i,j}^t)\right\|_2^2\right] \\
 &\leq\eta_t^2k\frac{1}{m}\sum_{i=1}^m\sum_{j=1}^k\mathbb{E}\left[\|\nabla f_i(\mathbf{w}_{i,j}^t,\xi_{i,j}^t)\|_2^2\right]\leq\eta_t^2k^2G^2, \quad (\text{by Assumption D.3}) \quad (28)
 \end{aligned}$$

and

$$\mathbb{E}\left[\left\|\eta_t\frac{s}{n}\nu\right\|_2^2\right]\leq\eta_t^2\frac{n^2}{s^2}\mathbb{E}\left[\sum_{j=1}^d\nu_j^2\right]\leq\eta_t^2\frac{n^2}{s^2}d\sigma_\nu^2. \quad (29)$$

We rewrite the third term on the RHS of (27) as follows:

$$\begin{aligned}
 2\mathbb{E}\left[\left\langle\mathbf{w}^t-\mathbf{w}^*,\frac{1}{m}\sum_{i=1}^m\Delta\mathbf{w}_i^t\right\rangle\right] &=2\eta_t\frac{1}{m}\sum_{i=1}^m\mathbb{E}\left[\left\langle\mathbf{w}^*-\mathbf{w}^t,\sum_{j=1}^k\nabla f_i(\mathbf{w}_{i,j}^t,\xi_{i,j}^t)\right\rangle\right] \\
 &=2\eta_t\frac{1}{m}\sum_{i=1}^m\mathbb{E}\left[\left\langle\mathbf{w}^*-\mathbf{w}^t,\nabla f_i(\mathbf{w}^t,\xi_{m,1}^t)\right\rangle\right] \\
 &\quad +2\eta_t\frac{1}{m}\sum_{i=1}^m\mathbb{E}\left[\left\langle\mathbf{w}^*-\mathbf{w}^t,\sum_{j=2}^k\nabla f_i(\mathbf{w}_{i,j}^t,\xi_{i,j}^t)\right\rangle\right]. \quad (30)
 \end{aligned}$$

To bound this term further, we need the following result. We observe the following:

$$\begin{aligned}
 &2\eta_t\frac{1}{m}\sum_{i=1}^m\mathbb{E}\left[\left\langle\mathbf{w}^*-\mathbf{w}^t,\nabla f_i(\mathbf{w}^t,\xi_{m,1}^t)\right\rangle\right] \\
 &=2\eta_t\frac{1}{m}\sum_{i=1}^m\mathbb{E}\left[\left\langle\mathbf{w}^*-\mathbf{w}^t,\nabla f_i(\mathbf{w}^t)\right\rangle\right] \quad (\text{since}\mathbb{E}_\xi[\nabla f_i(\mathbf{w}_{i,j}^t,\xi_{i,j}^t)]=\nabla f_i(\mathbf{w}_{i,j}^t),\forall i,m) \\
 &\leq2\eta_t\frac{1}{m}\sum_{i=1}^m\mathbb{E}\left[f_i(\mathbf{w}^*)-f_i(\mathbf{w}^t)-\frac{\mu}{2}\|\mathbf{w}^t-\mathbf{w}^*\|_2^2\right] \quad (\text{by Assumption D.2}) \\
 &=2\eta_t\left(f^*-\mathbb{E}[f(\mathbf{w}^t)]-\frac{\mu}{2}\mathbb{E}\left[\|\mathbf{w}^t-\mathbf{w}^*\|_2^2\right]\right)\leq-\mu\eta_t\mathbb{E}\left[\|\mathbf{w}^t-\mathbf{w}^*\|_2^2\right] \quad (\text{since}f^*\leq f(\mathbf{w}^t),\forall t) \quad (31)
 \end{aligned}$$

**Lemma E.1** ((Amiri et al., 2020), Lemma 2). *For  $0\leq\eta_t\leq 1$*

$$\begin{aligned}
 2\eta_t\frac{1}{m}\sum_{i=1}^m\mathbb{E}\left[\left\langle\mathbf{w}^*-\mathbf{w}^t,\sum_{j=2}^k\nabla f_i(\mathbf{w}_{i,j}^t,\xi_{i,j}^t)\right\rangle\right] &\leq-\mu\eta_t(1-\eta_t)(k-1)\mathbb{E}\left[\|\mathbf{w}^t-\mathbf{w}^*\|_2^2\right]+\eta_t^2(k-1)G^2 \\
 &\quad +\left(1+\mu(1-\eta_t)\right)\eta_t^2G^2\frac{k(k-1)(2k-1)}{6}+2\eta_t(k-1)\Gamma. \quad (32)
 \end{aligned}$$

Substituting the bound obtained from above lemma (31) and (32) in Equation (30), we obtain:

$$\begin{aligned}
 & 2\mathbb{E}\left[\left\langle \mathbf{w}^t - \mathbf{w}^*, \frac{1}{m} \sum_{i=1}^m \Delta \mathbf{w}_i^t \right\rangle\right] \\
 & \leq -\mu\eta_t(k - \eta_t(k - 1))\mathbb{E}\left[\|\mathbf{w}^t - \mathbf{w}^*\|_2^2\right] + \eta_t^2(k - 1)G^2 \\
 & \quad + (1 + \mu(1 - \eta_t))\eta_t^2G^2 \frac{k(k - 1)(2k - 1)}{6} + 2\eta_t(k - 1)\Gamma.
 \end{aligned} \tag{33}$$

Substituting the above inequality in Equation (28), leads to the following upper bound on  $\mathbb{E}[\|\mathbf{w}^{t+1} - \mathbf{w}^*\|_2^2]$ , when substituted into (27):

$$\begin{aligned}
 \mathbb{E}\left[\|\mathbf{w}^{t+1} - \mathbf{w}^*\|_2^2\right] & \leq (1 - \mu\eta_t(k - \eta_t(k - 1)))\mathbb{E}\left[\|\mathbf{w}^t - \mathbf{w}^*\|_2^2\right] + \eta_t^2(k^2 + k - 1)G^2 + \eta_t^2 d\sigma^2(t) \\
 & \quad + (1 + \mu(1 - \eta_t))\eta_t^2G^2 \frac{k(k - 1)(2k - 1)}{6} + 2\eta_t(k - 1)\Gamma.
 \end{aligned} \tag{34}$$

□

## F. Experimental Details

### F.1. Network Architecture and Experimental Settings

Table 2. CNN architecture for image classification on MNIST and CIFAR-10.

MNIST	CIFAR-10
5x5 kernel size, 32 channels	3x3 kernel size, 32 channels, ReLU activation
	3x3 kernel size, 32 channels, ReLU activation
2x2 max pooling	
5x5 kernel size, 64 channels	3x3 kernel size, 64 channels, ReLU activation
	3x3 kernel size, 64 channels, ReLU activation
2x2 max pooling	
fully connect layer with 512 units, ReLU activation	3x3 kernel size, 128 channels, ReLU activation
	3x3 kernel size, 128 channels, ReLU activation
softmax output layer with 10 units	

Table 3. Experiment settings

Network-Dataset	Clients	Samples/device	Clients/round	Optimizer	Batch size	Epoch
CNN-MNIST	100	600	10	SGD	100	5
CNN-CIFAR-10	10	5000	5	ADAM	100	5
RNN-Shakespeare	660	unbalanced	40	ADAM	50	5

### F.2. Pretrain Autoencoder

In this paper,  $d$  denotes the size of model parameters and gradient. Usually, the size of neural network is huge. It is too expensive to encode all the gradients at once through autoencoder, so we divide gradients into blocks with each block size of  $b$ . There are  $\lceil \frac{d}{b} \rceil$  blocks to be encoded.

We define block-wise encoder  $\bar{E}_c : \mathbb{Q}_s^b \rightarrow \mathbb{R}^{\frac{b}{2}}$  and decoder  $\bar{D}_c : \mathbb{R}^{\frac{b}{2}} \rightarrow \mathbb{Q}_s^b$ . Then, we implement  $(E_c, D_c)$  by:

$$\begin{aligned}
 E_c(\mathbf{l}) & \triangleq \text{Concatenate}(\bar{E}_c(\bar{\mathbf{l}}_1), \dots, \bar{E}_c(\bar{\mathbf{l}}_{\frac{d}{b}})), \\
 D_c(\mathbf{x}) & \triangleq \text{Concatenate}(\bar{D}_c(\bar{\mathbf{x}}_1), \dots, \bar{D}_c(\bar{\mathbf{x}}_{\frac{d}{b}})),
 \end{aligned}$$



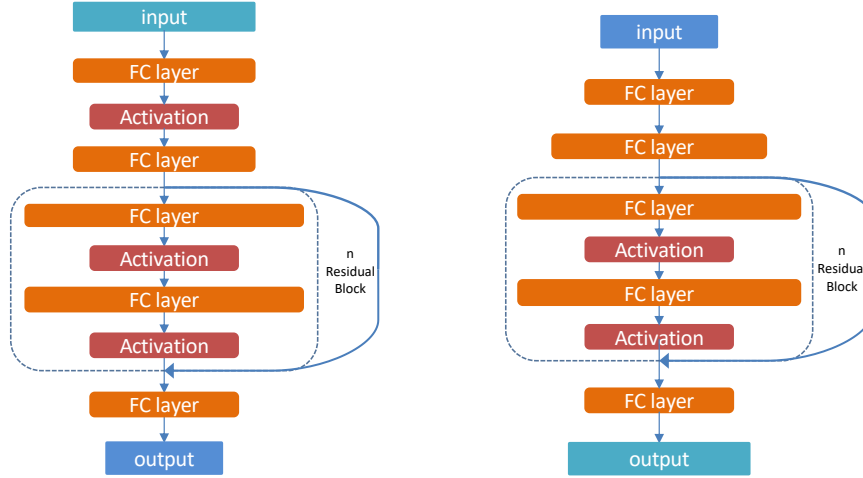


Figure 6. The architecture of encoder-decoder network used in this paper. The left one is the encoder. The right one is the decoder. The number of residual block is 3 for both encoder and decoder. Activation function is ReLU.

where  $\bar{l} \in \mathbb{Q}_s^b$  and  $\bar{x} \in \mathbb{R}^{\frac{b}{2}}$ . We randomly sample  $50,000m$  vectors from quantization domain  $\mathbb{Q}_s^b$  as train dataset  $\mathcal{D}_{train}^{b,s}$ . And  $10,000m$  samples from  $\mathbb{Q}_s^b$  as test dataset  $\mathcal{D}_{test}^{b,s}$ . For each epoch,  $\mathcal{D}_{train}^{b,s}$  will be shuffled at first. Every  $m$  samples taken from  $\mathcal{D}_{train}$  are a single inputs for training procedure following the objective function 7. We take the best  $(\bar{E}_c, \bar{D}_c)$  within 50 epochs is what achieved the least variance on  $\mathcal{D}_{test}$ . Adam optimizer with 0.0001 learning rate utilizes this training procedure.

In this section, we pretrain a few encode-decoder networks in the way we described above. The architecture of autoencoders are shown in Figure 6. To investigate the variance distribution of FedAGE, we generate 10,000 samples to observe the probability density curve of variance  $\nu$  (defined in 8). Then, we draw three different probability density function curve of Gaussian distribution with expectation 0 and standard variance  $\sigma = \sigma_\nu, \sigma_\nu/3$  and  $3\sigma_\nu$ . The results are shown in Figure 7 for the  $m = 5$  and Figure 8 for  $m = 10$ . The results indicate that the distribution of FedAGE variance is a hybrid Gaussian distribution. With the larger encoded domain (larger block size  $b$  and quantization level  $s$ ), the distribution becomes a Gaussian noise with expectation 0 and standard variance  $\sigma_\nu$ . By observing the different plot with same  $b, s$  in Figure 7 and Figure 8, we conclude that the more client in FedAGE scheme the smaller the variance  $\sigma_\nu$  is. This conclusion is consistent with the bound we analyzed in lemma 3.2.

### F.3. Gradient Inversion Visualization Results

Full results are shown in Table 4.

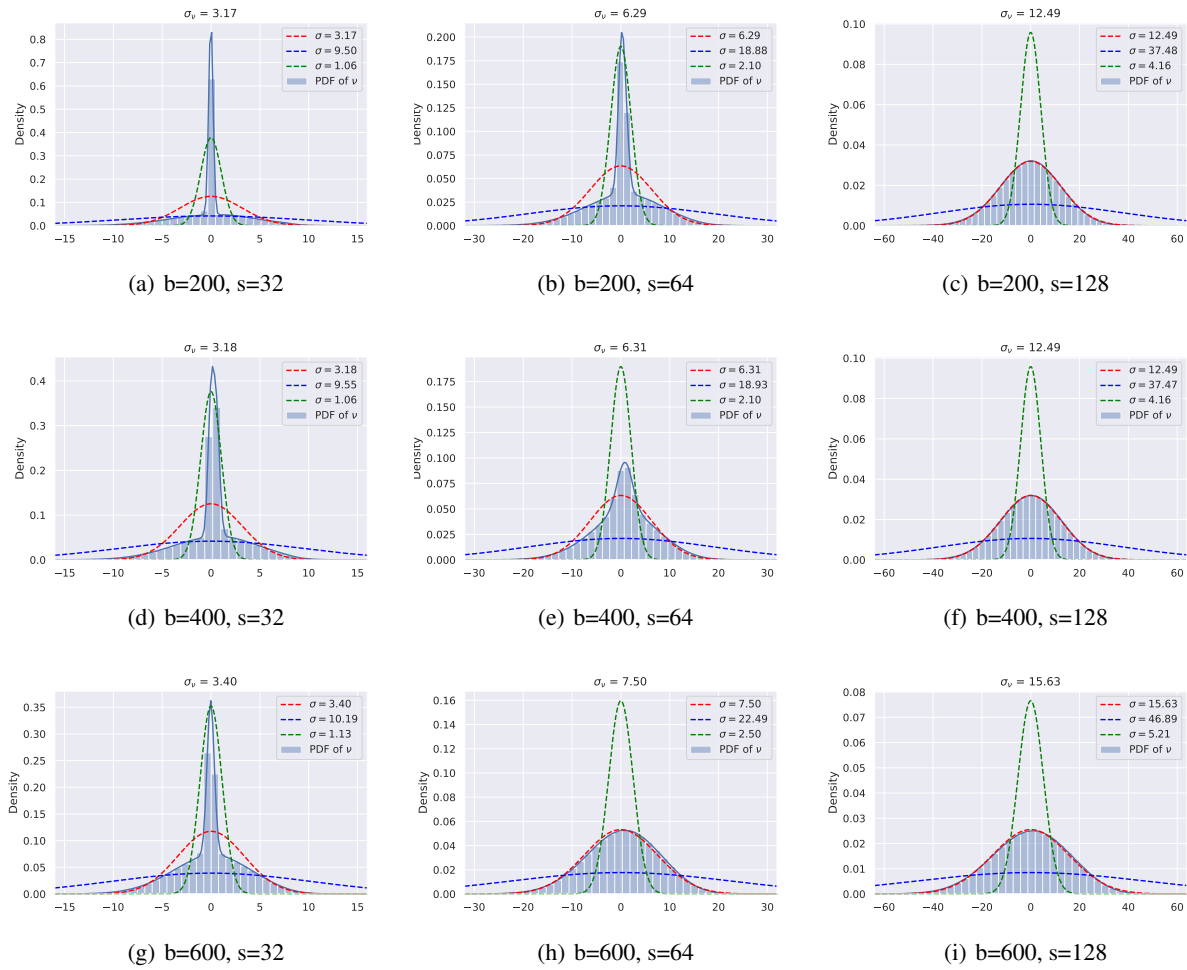
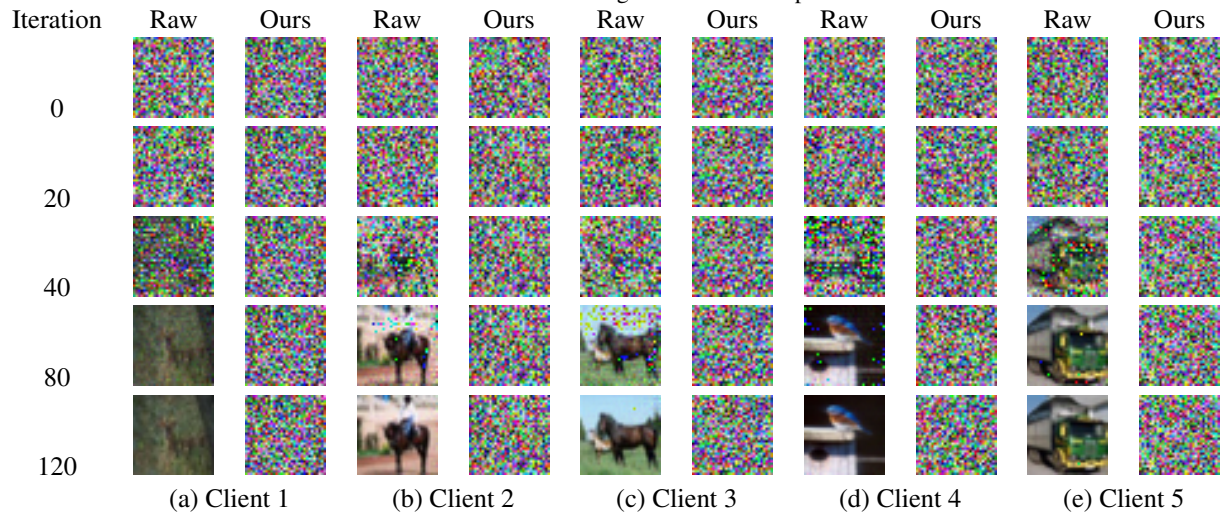


Figure 7. Distribution of aggregation noise with  $m=5$ .

Table 4. The visualization of gradient inversion procedure.



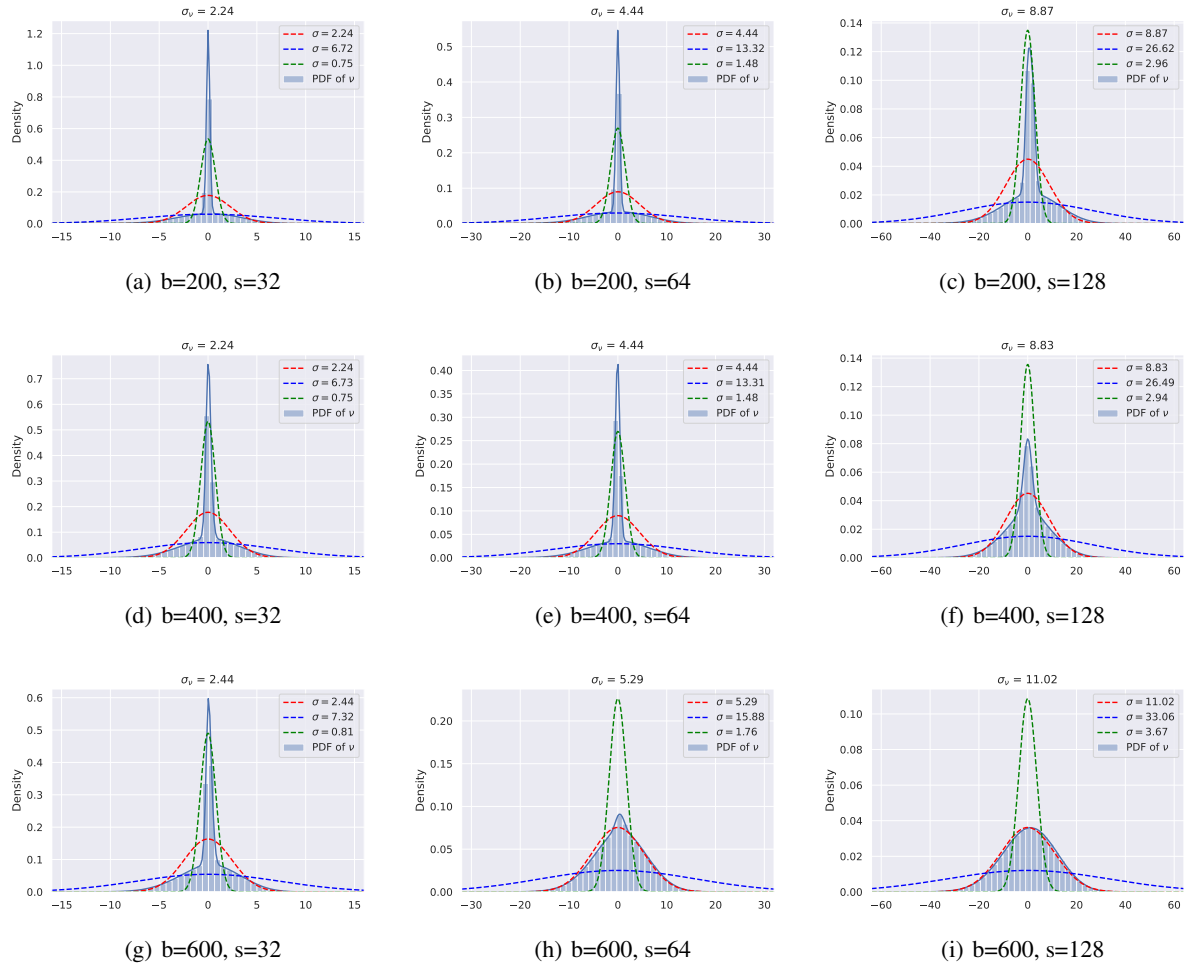


Figure 8. Distribution of aggregation noise with  $m=10$ .